Drug Design, Development and Therapy

Dovepress
open access to scientific and medical research

Open Access Full Text Article

ORIGINAL RESEARCH

Novel Phenolic Compounds as Potential Dual EGFR and COX-2 Inhibitors: Design, Semisynthesis, in vitro Biological Evaluation and in silico Insights

Mohamed A Abdelgawad,[1] Arafa Musa,[2] Atiah H Almalki,[3,4] Sami I Alzarea,[5] Ehab M Mostafa,[2] Mostafa M Hegazy,[6] Gomaa Mostafa-Hedeab,[7] Mohammed M Ghoneim,[6,8] Della GT Parambi,[1] Rania B Bakr,[1] Nayef S Al-Muaikel,[9] Abdullah S Alanazi,[10,11] Metab Alharbi,[12] Waqas Ahmad,[13] Syed NA Bukhari,[1] Mohammad M Al-Sanea[1]

[1]Department of Pharmaceutical Chemistry, College of Pharmacy, Jouf University, Sakaka, Aljouf, 72341, Saudi Arabia; [2]Department of Pharmacognosy, College of Pharmacy, Jouf University, Sakaka, 72341, Saudi Arabia; [3]Department of Pharmaceutical Chemistry, College of Pharmacy, Taif University, Taif, 21944, Saudi Arabia; [4]Addiction and Neuroscience Research Unit, Taif University, Taif, 21944, Saudi Arabia; [5]Department of Pharmacology, College of Pharmacy, Jouf University, Sakaka, Aljouf, 72341, Saudi Arabia; [6]Department of Pharmacognosy, Faculty of Pharmacy, Al-Azhar University, Cairo, 11371, Egypt; [7]Department of Pharmacology, Medical College, Jouf University, Sakaka, Aljouf, 72341, Saudi Arabia; [8]Department of Pharmacy Practice, College of Pharmacy, AlMaarefa University, Ad Diriyah, 13713, Saudi Arabia; [9]Department of Chemistry, College of Science, Jouf University, Sakaka, Aljouf, 72341, Saudi Arabia; [10]Department of Clinical Pharmacy, College of Pharmacy, Jouf University, Sakaka, Aljouf, Saudi Arabia; [11]Health Sciences Research Unit, Jouf University, Sakaka, Aljouf, Saudi Arabia; [12]Department of Pharmacology and Toxicology, College of Pharmacy, King Saud University, Riyadh, 11451, Saudi Arabia; [13]Drug and Herbal Research Centre, Faculty of Pharmacy, Universiti Kebangsaan Malaysia, Kuala Lumpur, Malaysia

Correspondence: Mohamed A Abdelgawad
Department of Pharmaceutical Chemistry, College of Pharmacy, Jouf University, Sakaka, Aljouf, 72341, Kingdom of Saudi Arabia
Tel +966 595435214
Email mohamedabdelwahab976@yahoo.com

Arafa Musa
Department of Pharmacognosy, College of Pharmacy, Jouf University, Sakaka, Aljouf, 72341, Kingdom of Saudi Arabia
Tel +966 558775403
Email akmusa@ju.edu.sa

Introduction: Epidermal growth factor receptor (EGFR) inhibition is an imperative therapeutic approach targeting various types of cancer including colorectal, lung, breast, and pancreatic cancer types. Moreover, cyclooxygenase-2 (COX-2) is frequently overexpressed in different types of cancers and has a role in the promotion of malignancy, apoptosis inhibition, and metastasis of tumor cells. Combination therapy has been emerged to improve the therapeutic benefit against cancer and curb intrinsic and acquired resistance.

Methods: Three semi-synthetic series of compounds (**C1-4**, **P1-4**, and **G1-4**) were prepared and evaluated biologically as potential dual epidermal growth factor receptor (EGFR) and COX-2 inhibitors. The main phenolic constituents of *Amaranthus spinosus* L. (*p*-coumaric, caffeic and gallic) acids have been isolated and subsequently subjected to diazo coupling with various amines to get novel three chemical scaffolds with potential anticancer activities.

Results: Compounds **C4** and **G4** showed superior inhibitory activity against EGFR (IC_{50}: 0.9 and 0.5 μM, respectively) and displayed good COX-2 inhibition (IC_{50}: 4.35 and 2.47 μM, respectively). Moreover, the final compounds were further evaluated for their cytotoxic activity against human colon cancer (HT-29), pancreatic cancer (PaCa-2), human malignant melanoma (A375), lung cancer (H-460), and pancreatic ductal cancer (Panc-1) cell lines. Interestingly, compounds **C4** and **G4** exhibited the highest cytotoxic activity with average IC_{50} values of 1.5 μM and 2.8 μM against H-460 and Panc-1, respectively. The virtual docking study was conducted to gain proper understandings of the plausible-binding modes of target compounds within EGFR and COX-2 binding sites.

Discussion: The NMR of prepared compounds showed characteristic peaks that confirmed the structure of the target compounds. The synthesized benzoxazolyl scaffold containing compounds showed inhibitory activities for both COXs and EGFR which are consistent with the virtual docking study.

Keywords: kinase inhibitors, anti-inflammatory, multitarget agents, BRAF, anticancer

Introduction

Phenolic compounds are considered as one of the most ubiquitously distributed phytochemicals; they are abundantly found in most vegetables and fruits and utilized as food supplement.[1,2] Most of them possess various pharmacological activities and can be therapeutically indicated as antioxidants,[3,4] anti-inflammatory,[5,6] antimicrobial,[7] antifungal,[8] antidiabetic,[9] and anticancer agents.[10] They can be classified chemically

Received: 12 March 2021
Accepted: 12 May 2021
Published: 31 May 2021

into curcuminoids (curcumin, tetrahydrocurcumin), stilbenes (resveratrol, pterostilbene), quinones (naphthoquinones, anthraquinones), lignans (sesamin, enterolactone), coumarins (umbelliferone, aesculetin), tannins (ellagitannins), flavonoids (silymarin, genistein, diosmin, quercetin) and simple phenolics (phenolic acids as caffeic and gallic acids).[11]

Cancer is considered one of the most dreadful diseases that lead to fatality; it is the second key reason for mortality after cardiovascular diseases.[12,13] The discovery of new and multitarget drugs for the treatment of cancer is of great importance due to the severity of the disease and the produced side effects of the already approved drugs. As oncogenic kinases play an important role in cell proliferation, inhibition or blocking of their actions has become an important strategy for cessation and termination of human malignancies.[14,15] Overexpression of COXs enzymes has been detected in different types of tumor and implicated in cancer progression.[16–19] Accordingly, the design and discovery of drugs possessing dual kinases and COXs enzymes inhibition are of great interest to prevent oncogenesis.[20]

Epidermal growth factor receptor (EGFR) is a receptor tyrosine kinase (RTK). It has crucial role in different cell physiological processes including proliferation, differentiation and migration. The extracellular domain of EFGR has the binding site for endogenous epidermal growth factors (EGF), which consequently induces a conformational change in the tyrosine kinase domain (TKD) in the wild type from an inactive to active state. However, $EGFR^{L858R}$ represents one of the most common oncogenic point mutation that make EGFR kinase constitutively active. EGFR has become a potential drug target for treatment of different human malignancies. Overexpression of mutant forms of EGFR was identified in various types of human carcinomas. Erlotinib is a competitive EGFR inhibitor. For $EGFR^{L858R}$, the point mutation does not affect negatively the affinity of the inhibitor to the kinase active site.[21–23]

Herein, we amend the naturally occurring active phytochemicals to develop novel chemical entities as a perusal of discovering new, multi-targeted drugs through various semi-synthetic step reactions.[19,24–27] Structural modification of plants secondary metabolites can enhance the biological activity of the parent compounds or augment the scope of their pharmacological activities. ÷n continuation of our efforts to find potent anti-cancer agents, new hybrid molecules were semi synthesized based on benzimidazole/benzoxazole moieties as they incorporated in many propitious oncogenic proteins inhibitors.[17,23,28–31] Through azo coupling reaction, benzimidazole and benzoxazole were chemically combined with naturally isolated phenolic compounds in three chemical scaffolds, which serve our target core structures (Figure 1). The COX-2 and EGFR inhibitory activities for all target compounds will be addressed. Moreover, in silico, study will be investigated for those compounds tested against EGFR tyrosine kinase using docking to elucidate a postulated model for their binding at the molecular level.

Materials and Methods

All cell lines used in this study, were purchased commercially, from the ECACC collection through local suppliers of Merck and Sigma-Aldrich and Cells were grown according to ECACC recommendations.

Extraction and Isolation

Five kilograms of the aerial parts of *Amaranthus spinosus L.* (*Amaranthaceae*) were thoroughly washed, shade dried, ground, defatted with n-hexane and extracted with ethyl ethanoate. The ethyl ethanoate extract (24 g) was divided on vacuum liquid chromatography (VLC) to afford five fractions (I–V). Based on the analytical high-performance liquid chromatography (HPLC) and liquid chromatography-mass spectroscopy (LC-MS) chromatograms, fractions II and V were selected for isolation and purification of their phenolic constituents.[12] After a series of chromatographic development for fractions II and V, the subfractions II_b and V_d were separately subjected to further isolation and purification on normal silica gel and Sephadex LH-20, followed by injection on preparative HPLC to obtain the target phenolic acids.[32] The HPLC was operating with a one-hour program, starting at 10% methanol in water for 5 min. For 45 min, a gradual increase of methanol concentration from 10% to 100%. The flow rate will then be maintained at 20 mL/min for 10 min with 10% MeOH. The retention times (t_R) were 16.13, 15.47, 14.58 min for p-coumaric acid (45 mg), caffeic acid (36 mg) and gallic acid (24 mg), respectively. Several runs have been performed per sample to obtain the required amounts for semi-synthesis of the target compounds.

Synthesis of Azo-Acid Derivatives (II)

To the mixture of aniline derivatives (0.01 mol) and HCl (conc, 5mL) in an ice bath, sodium nitrite solution (0.01 mol, 5mL distilled water) was added dropwise and stirred for 2h. The diazonium mixture was added to the phenolic

solution (0.01 mol) in NaOH (30% 10mL). The mixture was then neutralized using CH_3COONa (10%, H_2O). The separated dye was collected, filtered, and dried. The obtained dye was chromatographed on normal column silica gel using a mixture of DCM:CH_3OH solvent system. The prepared compounds were characterized as (**C1-4, P1-4** and, **G1-4**).

E-3-(2-(E) 4-Acetylphenyl)Diazenyl)-3,4-Dihydroxyphenyl)Acrylic Acid (C1)

mp: >300 °C; yield: 75%; yellow powder (MeOH); ^{1}HNMR: δ 7.94 (2H, d, *J*=8.4 Hz, acetophenone H-3`, 5`), 7.69 (2H, d, *J*=8.0 Hz, acetophenone H-2`, 6`), 7.29 (1H, d, *J*=16.4 Hz, CH=CHCOOH), 7.04 (1H, d, *J*=16.4 Hz, CH=CHCOOH), 6.95 (1H, d, *J*=8.0 Hz, caffeic H-5), 6.78 (1H, d, *J*=8.0 Hz, caffeic H-6), 2.51 (3H, s, CH_3); ^{13}CNMR: δ 197.62 (C=O, acetyl), 171.23 (COOH), 146.76, 145.97, 142.83, 135.39, 132.24, 129.2, 128.67, 126.52, 124.29, 119.70, 116.23, 114.15, 27.26 (CH_3); EIMS: m/z (%): 326 (19.16) $[M]^+$. Anal. Calcd. for $C_{17}H_{14}N_2O_5$: C, 62.57; H, 4.32; N, 8.59. Found: C, 62.50; H, 4.30; N, 8.50.

(E)-3-(3-((E)-(4-Acetylphenyl)Diazenyl)-4-Hydroxyphenyl)Acrylic Acid (P1)

mp: > 300°C; yield: 64%; yellow powder (MeOH); ^{1}HNMR: δ 8.12 (2H, d, *J*=8.1 Hz, acetophenone H-3`, 5`), 7.97 (2H, d, *J*=8.0 Hz, acetophenone H-2`, 6`), 7.65 (1H, brs, *p*-coumaric H-2), 7.45 (1H, dd, *J*=8.0, 1.5 Hz, *p*-coumaric H-6), 7.35 (1H, d, *J*=16.0 Hz, CH=CHCOOH), 6.85 (1H, d, *J*=8.1 Hz, *p*-coumaric H-5), 6.45 (1H, d, *J*=16.1 Hz, CH=CHCOOH), 2.52 (3H, s, CH_3); ^{13}CNMR: δ 198.03 (C=O, acetyl), 168.31 (COOH), 160.64, 152.51, 145.47, 139.07, 138.34, 130.57, 130.34, 126.92, 125.56, 122.03, 120.35, 117.48, 27.43 (CH_3); EIMS: m/z (%): 310 (28.78) $[M]^+$. Anal. Calcd. for $C_{17}H_{14}N_2O_4$: C, 65.80; H, 4.55; N, 9.3. Found: C, 65.70; H, 4.60; N, 9.00

2-{(4-Acetylphenyl)Diazenyl}-3,4,5-Trihydroxybenzoic Acid (G1)

mp: > 300°C; yield: 71%; Yellow powder (MeOH); ^{1}HNMR: δ 8.15 (2H, d, *J*=8.3 Hz, acetophenone H-3`, 5`), 7.85 (2H, d, *J*=8.1 Hz, acetophenone H-2`, 6`), 7.32 (1H, s, gallic H-6), 2.52 (3H, s, CH_3); ^{13}CNMR: δ 198.06 (C=O, acetyl), 169.63 (COOH), 151.70, 146.24, 141.12, 139.28, 138.19, 134.31, 130.12, 124.25, 118.61, 111.72, 27.26 (CH_3); EIMS: m/z (%): 316 (48.6) $[M]^+$. Anal. Calcd. for $C_{15}H_{12}N_2O_6$ (316): C, 56.96; H, 3.82; N, 8.86. Found: C, 56.90; H, 3.80; N, 8.90

E-3-(2-(E) 3-Acetylphenyl)Diazenyl)-3,4-Dihydroxyphenyl)Acrylic Acid (C2)

mp: > 300°C; yield: 60%; Yellow powder (MeOH); ^{1}HNMR: δ 8.11–8.07 (1H, m, acetophenone H-2`), 7.97–7.89 (1H, m, acetophenone H-4`), 7.92–7.87 (1H, m, acetophenone H-6`), 7.79–7.73 (1H, m, acetophenone H-5`), 7.24 (1H, d, *J*=16.4 Hz, CH=CHCOOH), 7.04 (1H, d, *J*=16.4 Hz, CH=CHCOOH), 6.79 (1H, d, *J*=8.2 Hz, caffeic H-5), 6.77 (1H, d, *J*=8.2 Hz, caffeic H-6), 2.52 (3H, s, CH_3); ^{13}CNMR: δ 198.61 (C=O, acetyl), 171.65 (COOH), 146.37, 145.92, 141.70, 134.52, 130.84, 129.49, 128.87, 127.33, 124.54, 119.34, 116.19, 115.36, 27.34 (CH_3); EIMS: m/z (%): 326 (66.69) $[M]^+$. Anal. Calcd. for $C_{17}H_{14}N_2O_5$: C, 62.75; H, 4.32; N, 8.59. Found: C, 62.60; H, 4.20; N, 8.70

(E)-3-(3-((E)-(3-Acetylphenyl)Diazenyl)-4-Hydroxyphenyl)Acrylic Acid (P2)

mp: >300°C; yield: 73%; yellow powder (MeOH); ^{1}HNMR: δ 8.11 (1H, m, acetophenone H-2`), 7.97–7.93 (2H, m, acetophenone H-4`,6`), 7.79–7.70 (1H, m, acetophenone H-5`), 7.50 (1H, dd, *J*=8.0, 1.5 Hz, *p*-coumaric H-6), 7.35 (1H, brs, *p*-coumaric H-2), 7.18 (1H, d, *J*=16.2 Hz, CH=CHCOOH), 6.79 (1H, d, *J*=8.1 Hz, *p*-coumaric H-5), 6.57 (1H, d, *J*=16.1 Hz, CH=CHCOOH), 2.54 (3H, s, CH_3); ^{13}CNMR: δ 197.95 (C=O, acetyl), 171.23 (COOH), 158.37, 157.57, 142.82, 139.25, 135.44, 131.83, 130.93, 129.22, 128.88, 126.50, 124.42, 123.41, 122.55, 118.19, 116.59, 116.13, 115.79, 27.10 (CH_3); EIMS: m/z (%): 310 (28.71) $[M]^+$. Anal. Calcd. for $C_{17}H_{14}N_2O_4$: C, 65.80; H, 4.55; N, 9.3. Found: C, 65.80; H, 4.50; N, 9.10

2-{(3-Acetylphenyl)Diazenyl}-3,4,5-Trihydroxybenzoic Acid (G2)

mp: > 300°C; yield =74%; yellow powder (MeOH); ^{1}HNMR: δ 8.18–8.16 (2H, m, acetophenone H-2`, 4`), 8.05–8.02 (1H, m, acetophenone H-6`), 7.72–7.70 (1H, m, acetophenone H-5`), 7.12 (1H, s, gallic H-6), 2.51 (3H, s, CH_3); ^{13}CNMR: δ 197.80 (C=O, acetyl), 168.83 (COOH), 152.11, 147.15, 142.12, 139.55, 136.42, 133.28, 130.98, 127.91, 126.82, 123.43, 116.24, 110.15, 26.86 (CH_3); EIMS: m/z (%): 316 (72.7) $[M]^+$. Anal. Calcd. for $C_{15}H_{12}N_2O_6$: C, 56.96; H, 3.82; N, 8.86. Found: C, 57.00; H, 3.70; N, 8.89

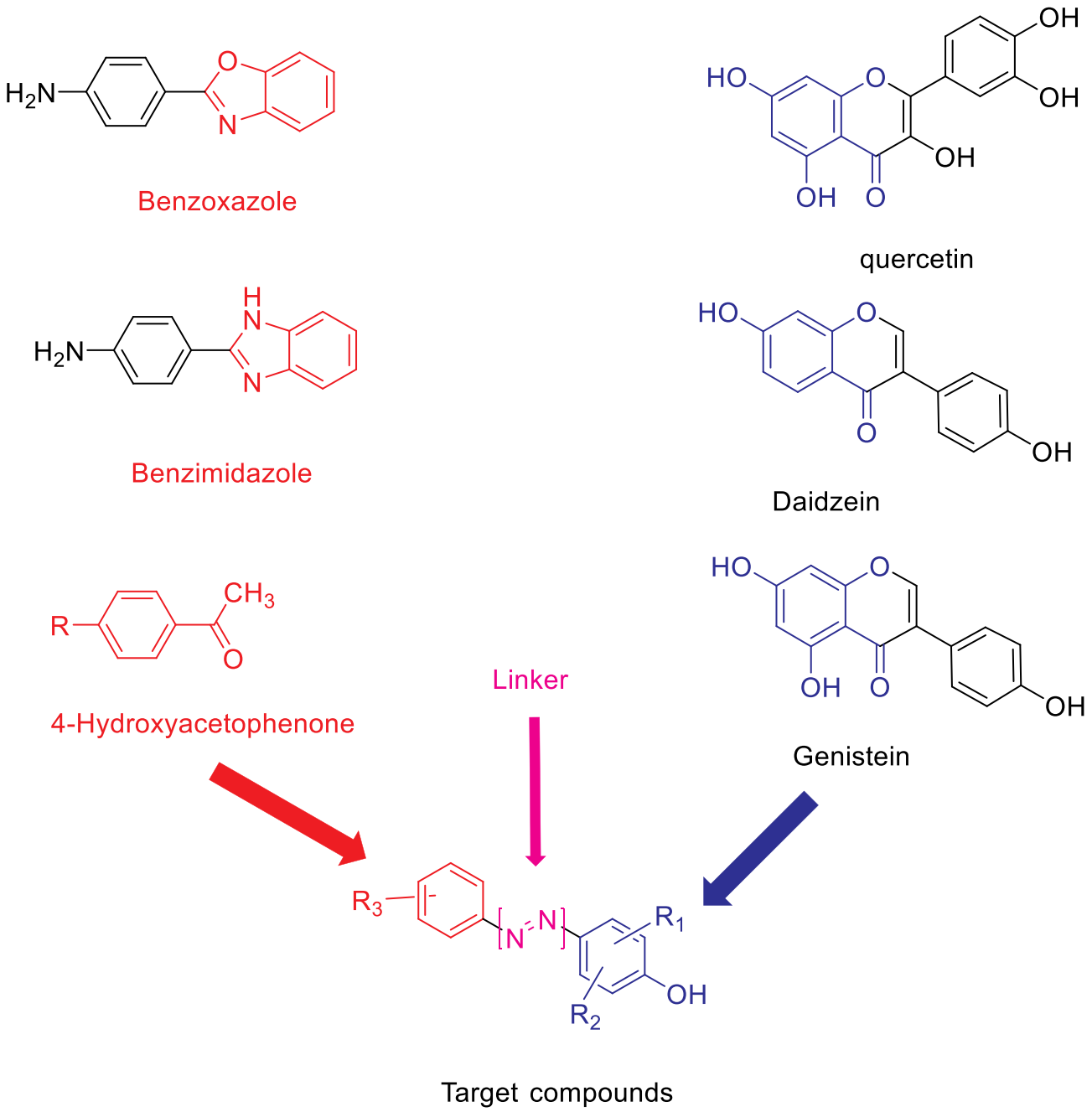

Figure 1 Scaffold of the target compounds.

E-3-(2-(E)-3-(1H Benzo[D]Imidazo-2-Yl)Phenyl) Diazenyl)-3,4-Dihydroxyphenyl)Acrylic Acid (C3)

mp: > 300°C; yield = 50%; yellow powder (MeOH); ^{1}HNMR: δ 8.32–8.26 (2H, m, phenyl H-2`, 4`), 7.99 (1H, d, *J*=16.1 Hz, CH=CHCOOH), 7.82–7.77 (2H, m, phenyl H-5`-6`), 7.60–7.25 (4H, m, Benzoimidazol), 6.93 (1H, d, *J*=8.1 Hz, caffeic H-5), 6.82 (1H, d, *J*=8.1 Hz, caffeic H-6), 6.71 (1H, d, *J*=16.1 Hz, CH=CHCOOH); ^{13}CNMR: δ 172.64 (COOH), 153.82, 152.74, 148.37, 146.43, 141.64, 138.82, 138.56, 129.96, 129.71, 129.58, 123.01, 122.98, 121.88, 120.67, 120.42, 119.37, 116.45, 115.13; EIMS: m/z (%): 400 (60.30) $[M]^{+}$. Anal. Calcd. for $C_{22}H_{16}N_4O_4$: C, 66.00; H, 4.03; N, 13.99. Found: C, 66.1; H, 4.00; N, 14.00

E-3-(3-(E) 3-(1H Benzo[D]Imidazol-2-Yl)Phenyl) Diazenyl)-4-Hydroxyphenyl)Acrylic Acid (P3)

mp: > 300°C; yield: 62%; yellow powder (MeOH); ^{1}HNMR: δ 8.35–8.30 (2H, m, phenyl H-2`, 4`), δ 8.03–

7.98 (2H, m, phenyl H-5`, 6`), 7.75 (1H, d, *J*=16.0 Hz, CH=CHCOOH), 7.65–7.27 (4H, m, Benzo-imidazlolyl), 7.63 (1H, d, *J*=8.0 Hz, *p*-coumaric H-5), 7.41 (1H, dd, *J*=8.0, 1.6 Hz, *p*-coumaric H-6), 6.88 (1H, d, *J*= 1.6 Hz, *p*-coumaric H-2), 6.65 (1H, d, *J*=16.0 Hz, CH=CHCOOH); ^{13}CNMR: δ 171.51 (COOH), 153.22, 152.84, 150.76, 147.31, 141.61, 132.80, 125.43, 130.64, 129.94, 129.70, 129.52, 123.06, 122.95, 121.87, 120.61, 120.01, 116.51, 115.22; EIMS: m/z (%): 384 (37.19) $[M]^+$. Anal. Calcd. for $C_{22}H_{16}N_4O_3$: C, 68.74; H, 4.20; N, 14.58. Found: C, 68.70; H, 4.30; N, 14.50

E)-2-{3-(1H-Benzo[B]Imidazole-2-Yl)Phenyl) Diazenyl)-3,4,5-Trihydroxybenzoic Acid (G3)

mp: > 300°C; yield: 45%: yellow powder (MeOH); ^{1}HNMR: δ 8.37–8.30 (2H, m, phenyl H-2`4`), δ 8.01–7.97 (2H, m, phenyl H-5`6`), 7.70–7.25 (4H, m, Benzoimidazol), 7.22 (1H, s, gallic H-6); ^{13}CNMR: δ 168.67 (COOH), 152.65, 152.84, 149.87, 141.70, 141.11, 140.43, 134.61, 130.91, 129.62, 129.45, 122.81, 122.67, 121.73, 114.95, 113.24, 109.65; EIMS: m/z (%): 390 (68.04) $[M]^+$. Anal. Calcd. for $C_{20}H_{14}N_4O_5$: C, 61.54; H, 3.62; N, 14.35. Found: C, 61.60; H, 3.60; N, 14.40

E-3-(2-(E) 3-(Benzo[D]Oxazol-2-Yl)Phenyl) Diazenyl)-3,4-Dihydroxyphenyl)Acrylic Acid (C4)

mp: > 300°C; yield: 55%; yellow powder (MeOH); ^{1}HNMR: δ 8.27–8.20 (1H, m, phenyl H-2`), δ 8.15–8.11 (1H, m, phenyl H-4`), 8.01–7.97 (1H, m, phenyl H-6`), 7.89 (1H, d, *J*=16.1 Hz, CH=CHCOOH), δ 7.84–7.78 (1H, m, phenyl H-5`), 7.75–7.36 (4H, m, Benzo-oxazolyl), 7.02 (1H, d, *J*=8.2 Hz, caffeic H-5), 6.91 (1H, d, *J*=8.2 Hz, caffeic H-6), 6.24 (1H, d, *J*=16.1 Hz, CH=CHCOOH); ^{13}CNMR: δ 172.15 (COOH), 162.71, 153.22, 150.01, 148.92, 146.76, 141.51, 138.79, 138.61, 129.76, 129.56, 126.51, 124.88, 123.81, 123.05, 121.95, 120.67, 120.40, 119.48, 116.52, 119.13, 111.43; EIMS: m/z (%): 401 (25.33) $[M]^+$. Anal. Calcd. for $C_{22}H_{15}N_3O_5$: C, 65.83; H, 3.77; N, 10.47. Found: C, 65.70; H, 3.80; N, 10.50

E-3-(3-(E) 3-(Benzo[D]Oxazol-2-Yl)Phenyl) Diazenyl)-4-Hydroxyphenyl)Acrylic Acid (P4)

mp: > 300°C; yield: 65%; yellow powder (MeOH); ^{1}HNMR: δ 8.27–8.22 (1H, m, phenyl H-2`), δ 8.15–8.10 (1H, m, phenyl H-4`), 8.01–7.95 (1H, m, phenyl H-6`), 7.89 (1H, d, *J*=16.1 Hz, CH=CHCOOH), 7.84–7.80 (1H, m, *phenyl* H-5`), 7.75–7.36 (4H, m, Benzo-oxazolyl), 7.61 (1H, d, *J*=8.1 Hz, *p*-coumaric H-5), 7.38 (1H, dd, *J*=8.1, 1.6 Hz, *p*-coumaric H-6), 6.92 (1H, d, *J*= 1.6 Hz, *p*-coumaric H-2), 6.18 (1H, d, *J*=16.1 Hz, CH=CHCOOH); ^{13}CNMR: δ 172.45 (COOH), 162.82, 152.91, 150.12, 148.55, 146.61, 141.34, 132.02, 129.76, 129.70, 129.56, 126.51, 125.61, 124.88, 123.81, 123.05, 121.85, 120.50, 119.27, 116.39, 118.92, 111.24; EIMS: m/z (%): 385 (18.07) $[M]^+$. Anal. Calcd. for $C_{22}H_{15}N_3O_4$: C, 68.57; H, 3.92; N, 10.9. Found: C, 68.50; H, 4.00; N, 10.8

(E)-2-{3-(1H-Benzo[B]Oxazol-2-Yl)Phenyl)Diazenyl)-3,4,5-Trihydroxybenzoic Acid (G4)

mp: > 300°C; yield =54%; Yellow powder (MeOH); ^{1}HNMR: δ 8.26–8.23 (2H, m, phenyl H-2`4`), δ 7.87–7.83 (2H, m, phenyl H-5`H-6`), 7.74–7.35 (4H, m, Benzo-oxazolyl), 7.15 (1H, s, gallic H-6); ^{13}CNMR: δ 167.85 (COOH), 162.51, 152.73, 149.87, 147.46, 140.96, 139.12, 133.75, 129.34, 129.12, 126.02, 124.25, 123.34, 122.82, 121.30, 118.85, 113.40, 119.76, 108.85; EIMS: m/z (%): 391 (29.47) $[M]^+$. Anal. Calcd. for $C_{20}H_{13}N_3O_6$: C, 61.38; H, 3.35; N, 10.74. Found: C, 61.40; H, 3.30; N, 10.70

Cytotoxicity Assay

Determination of the cytotoxic effect of the target compounds was performed to assess their ability to kill the tumor cells, which reflects the anticancer activity of the tested compounds.[33,34] A known cytotoxic agent (Erlotinib) was selected as a reference standard. Various cell lines were applied in this test, as mentioned in the Supplementary Data.

EGFR and BRAF Inhibitory Activities

To assess the mechanism of action for the tested compounds as potential EGFR and BRAF inhibitors, all target compounds and Erlotinib were subjected experimentally to the kinase screening protocol according to the previously reported procedure (Table 1).3[35,36] 3 More details are available in the Supplementary Data.

Assay of Secretory PLA2-V Activity

Ellman's photometric assay was followed to assess secretory PLA2 activity.[37] (See Supplementary Data)

Cyclooxygenase Assay

A commercially available kit was used for the determination of azo-compounds activities on COX-1 and COX-2, which assessed the quantity of prostaglandin E2 (PGE2). The obtained data were shown in contrast to the control (solvent-treated sample). The test was performed in

Table 1 Effects of Compounds on $BRAF^{V600E}$ and EGFR

Compound	BRAF Inhibition IC_{50} ± SEM (μM)	EGFR Inhibition IC_{50} ± SEM (μM)
C4	5.8±1.3	0.9±0.3
G4	5.4±0.6	0.5±0.2
Erlotinib	0.07±0.02	0.05±0.02

triplicate, and the findings generally agreed within 10%. The assay was done according to reported methods (Table 2).[38–40] (See Supplementary Data)

Cell Treatment and ELISA Assay for IL-6 and TNF-α

The assay methods for IL-6 and TNF-α were adapted according to reported methods (Table 3).[41] (See Supplementary Data)

Statistical Analysis

ANOVA (One-way analysis of variance) was performed to investigate all the statistics. $P < 0.05$ was considered statistically significant.

Virtual Docking Study

The crystal structures of the COX-2 isoform and EGFR were obtained from the PDB (COX-2 ID: 1CX2 and EGFR ID: 5UGB). Identification of key amino acids required for inhibitory activity of enzymes' ligands were identified. Molecular Operating Environment (MOE, Version 2010) was applied for protein preparation and docking procedure of test compounds (Table 4). All energy minimizations were carried out with MOE until an RMSD gradient of 0.05 $kcal \cdot mol^{-1}Å^{-1}$ with MMFF94x force field and the partial charges were automatically calculated. For docking preparation, the water molecules in the proteins' crystal structures were removed and followed by the protonation using Protonate 3D protocol in MOE using the Triangle Matcher placement method and London dG scoring function. The co-crystallized ligands were used to define the binding site for docking and the essential binding modes.[35,42,43]

Docking Validation

Docking protocols were validated for both receptors through re-docking of the co-crystallized ligands and reproducing all original binding modes between the co-crystallized ligands and the two receptors' pockets in the vicinity of the binding sites. For COX-2, a docking pose with an energy score (S) = −11.99 kcal/mol and an RMSD of 0.574 Å from the co-crystallized ligand pose. For

Table 2 Inhibition of Secretory PLA_2-V, COX-1, COX-2

Compound	sPLA$_2$-V IC_{50} (μM)	COX-1 IC_{50} (μM)	COX-2 IC_{50} (μM)	Selectivity Index (SI)
C1	19.47±1.94	55.04±1.29	12.29±1.28	4.47
C2	19.35±1.76	53.12±2.14	12.25±1.05	4.33
C3	23.27±1.80	16.19±1.80	4.95±1.30	3.27
C4	22.57±1.69	16.55±1.82	4.35±1.87	3.80
P1	42.51±2.65	ND	>100	–
P2	43.91±2.80	ND	>100	–
P3	17.45±1.79	65.21±3.51	>100	–
P4	17.50±1.80	67.34±2.26	>100	–
G1	7.15±2.59	3.13±0.65	6.11±1.14	0.51
G2	8.47±1.25	2.19±0.97	5.51±1.27	0.39
G3	6.52±1.05	8.69±1.47	4.19±1.76	2.07
G4	5.68±0.54	9.87±1.54	2.47±1.97	3.99
Caffeic acid	26.84±1.09	22.86±1.29	8.58±1.18	2.66
p-coumaric acid	55.12±1.33	>100	>100	—
Gallic acid	9.79±1.54	46.08±1.06	8.14±1.37	5.66
Dexamethasone	0.57±0.06	-	-	—-
Indomethacin*	-	0.27±0.04	3.29±0.5	0.08

Notes: *30 μM concentration, values are the mean ± SD; n = 3.

Table 3 Inhibition of IL-6 and TNF-α

Compound	% Inhibition of IL-6	Relative Amount of LPS	% Inhibition of TNF-α	Relative Amount of LPS
G2	43	57	48	52
G3	29	71	32	68
G4	56	44	61	39
LPS Control	0	100	0	100

Table 4 Docking Results of **C4** with 5UGB and 1CX2

Compound No.	Energy Score Kcal/mol	Types of Interaction	Enzyme (Protein PDB)	Amino Acid Residue	Functional Group
C4	−13.8376	HB	EGFR (5UGB)	Met793	C=O
8BM (ligand)	−11.2500	HB	EGFR (5UGB)	Met793	N of imidazole
G4	−24.1500	HB HB HB HB Arene-cation interaction	COX-2 (1CX2)	His90 Tyr355 Ser530 Ser530 Arg513	N of bezoxazole C=O 3 OH 4 OH Phenyl ring
Bromocelecoxib	−13.8924	HB	COX-2 (1CX2)	His90	SO_2

EGFR, a docking pose with an energy score (S)= −13.874 kcal/mol and an RMSD of 0.774 Å from the co-crystallized ligand pose were observed.

Results and Discussion

Chemistry

The first set of target compounds (**C1-2, G1-2** and **P1-2**) were synthesized starting from 3 (and 4)-aminoacetophenones which are commercially available (Scheme 1). However, the second set of target compounds (**C3-4, G3-4** and **P3-4**) were synthesized from amino-imidazole (**B1)** and amino-oxazole (**B2**) which were prepared via condensation reaction of *o*-phenylene diamine (and 2-aminophenol) with 3-aminobenzoic acid using polyphosphoric acid as dehydrating agent (Scheme 2). All target compounds were finally prepared through diazotization and coupling reaction using sodium nitrite in presence of HCl to afford diazonium salts, which simultaneously added to a basic solution of phenolic acids to produce the target compounds **C, P** and **G**. The structure elucidation of newly synthesized compounds **P1-4, C1-4, G1-4** was done using nuclear magnetic resonance (NMR) and mass spectroscopy (MS) in addition to the elemental analysis. ^{1}HNMR peaks of compounds **P1-2, C1-2, G1-2** showed aliphatic peaks at δ range of 2.51–2.54 indicating the presence of acetyl groups. The number of aromatic protons' peaks was increased equivalent to the newly added phenyl ring. Also, doublet peaks equivalent to alkene groups of azo-caffeic derivatives (**C1-4**) appeared at 7.04–7.99 ppm with J coupling constant range as 16.1–16.4 Hz and azo-coumaric derivatives (**P1-4**) appeared at δ 6.45 −7.89 ppm with *J* coupling of 16–16.2 Hz. These *J* coupling data confirmed the *E* configuration of the prepared compound. ^{13}CNMR of new synthetic compounds showed characteristic peaks of carbonyl groups at δ 197.35 to 198.61 (for the acetyl group) and at 167.85 to 172.64 (for the carboxylic group).

Cytotoxic Activity

MTT cytotoxic assay was conducted on tested compounds for human colon cancer (HT-29), pancreatic cancer (PaCa-2), Human malignant melanoma (A375), Lung cancer (H-460), and Pancreatic ductal cancer (Panc-1) cell lines. The IC_{50} for all compounds was expressed in μM (Table 5). Compounds **C1-3, G1-3** displayed moderate activity on all tested cell lines, while **C4** and **G4** exhibited a potent effect on all tested cell lines, particularly H-460 (1.7 and 2.7 μM, respectively) and Panc-1 (1.3 and 3 μM, respectively) (Table 5). The potent cytotoxic activity derived because of diazo coupling between benzimidazole and/or benzoxazole with caffeic and/or gallic acids which are new scaffolds amended in this experiment.

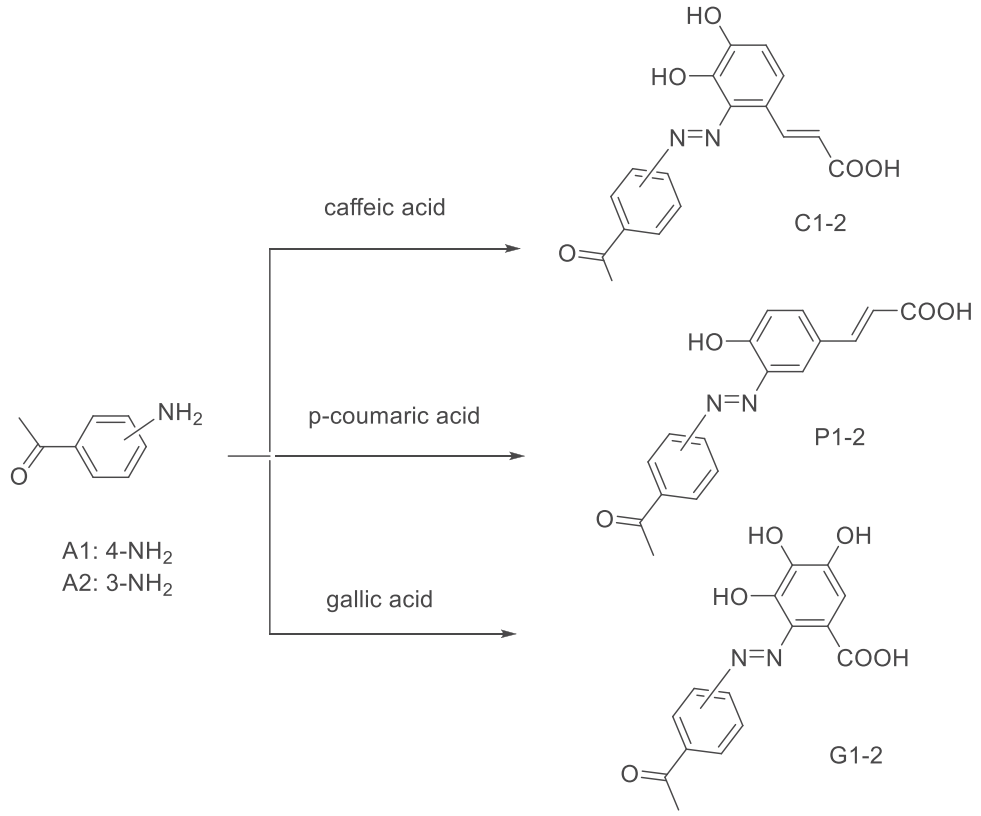

Scheme 1 Synthesis of compounds C1-2, G1-2 and P1-2; Conditions and reagents; HCl, and Sodium nitrite, at zero oC, added to phenolic acid in NaOH 10%, stirring for 48h, ice bath.

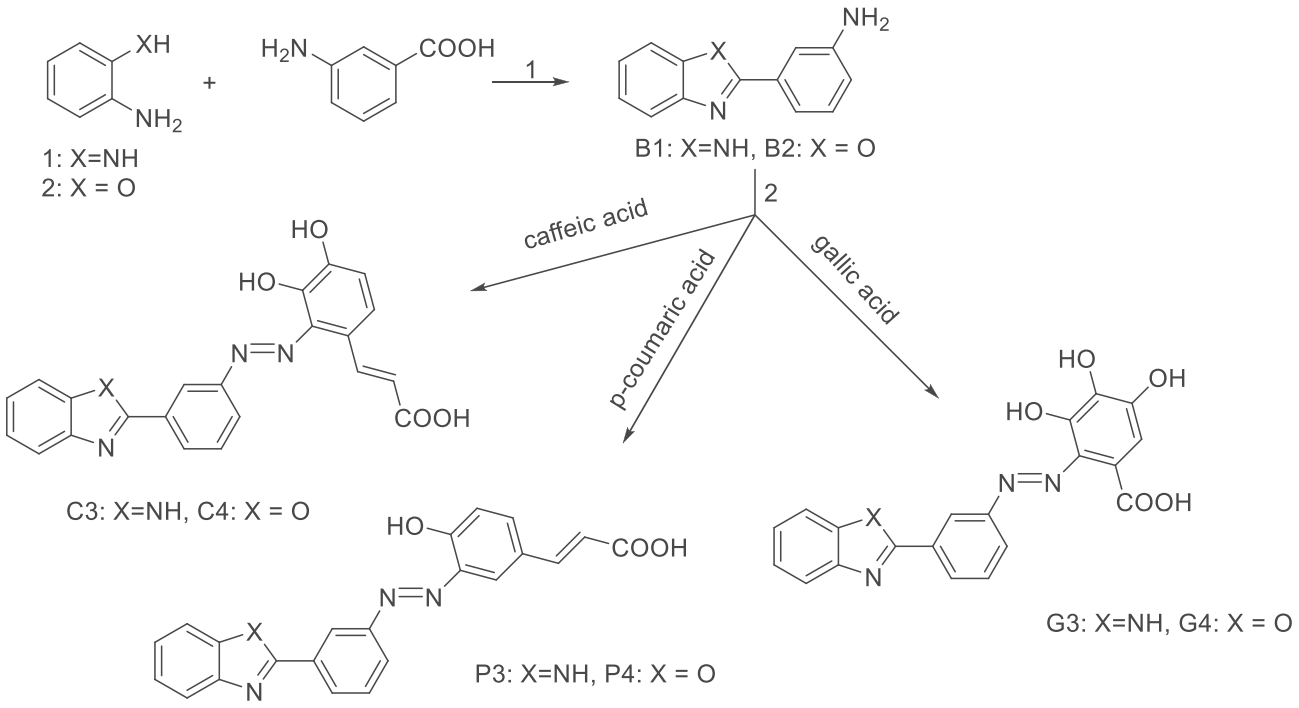

Scheme 2 Synthesis of compounds C3-4, G3-4 and P3-4; Conditions and reagents; 1) polyphosphoric acid, stirred for 4h at 220 oC, Na2CO3, crystallization from EtOH. 2) HCl, and Sodium nitrite, at zero oC, added to phenolic acid in NaOH 10%, stirring for 48h, ice bath.

Table 5 Effects of Tested Samples on Cell Lines

Code	Cell Viability %	Antiproliferative Activity IC_{50} ± SEM (μM)				
		HT-29	PaCa-2	A375	H-460	Panc-1
C1	97.3±1.4	>50	>50	>50	>50	>50
C2	98.0±1.2	>50	>50	>50	>50	>50
C3	98.1±1.4	9.4±1.2	8.6±1.2	12.1±2.8	8.9±1.2	12.5±1.5
C4	91.4±1.0	2.5±1.1	2.9±0.7	3.0±1.5	1.7±0.5	1.3±0.9
P1	97.9±1.2	>50	>50	>50	>50	>50
P2	97.4±1.8	>50	>50	>50	>50	>50
P3	98.2±1.6	>50	>50	>50	>50	>50
P4	98.1±1.4	>50	>50	>50	>50	>50
G1	85.4±1.6	14.6±2.8	12.0±1.7	12.9±1.2	13.6±1.2	12.7±1.8
G2	91.3±1.6	10.2±1.4	9.6±1.2	11.9±2.7	9.5±1.2	9.2±1.4
G3	85.2±1.5	12.4±1.8	13.4±1.6	14.8±2.4	12.2±1.4	13.8±2.4
G4	92.1±1.2	4.1±1.2	3.7±2.0	3.9±0.5	2.7±0.5	3.0±0.7
Caffeic acid	91.6±1.2	4.3±1.3	5.1±0.9	4.8±1.4	3.9±0.8	4.1±0.6
p-coumaric acid	97.9±1.2	>50	>50	>50	>50	>50
Gallic acid	98.3±1.7	16.3±1.6	17.5±1.3	18.7±2.2	14.9±1.2	17.9±1.4
Erlotinib	-	0.07±0.04	0.06±0.04	4.14±1.2	0.04±0.02	0.05±0.02

Protein Kinase Inhibition Activity

The targets were evaluated for their kinase inhibitory effect on BRAF and EGFR to explore their cytotoxic mechanism on the tested cell lines. Compounds **C4** and **G4** exhibited potent kinase inhibitory activity against BRAF (5.8±1.3 and 5.4±0.6 μM, respectively) and EGFR (0.9±0.3 and 0.5±0.2 μM, respectively), in comparison to the standard Erlotinib drug (IC_{50} = 0.07 and 0.05 μM, respectively) (Table 1).

Inhibition of Secretory PLA2-V, COX-1, COX-2 by Tested Compounds

Ellman's method-based assay was applied to assess the in vitro inhibitory activity against sPLA2 of the preparation at doses ranging from 1.25 to 20 μg/mL and the results are shown in Table 2. Dexamethasone was a positive control, and the inhibitory activities of targets azo-compounds against sPLA2-V observed IC_{50}: were in the range of 43.91 (P2) to 5.68 uM (**G4**). The

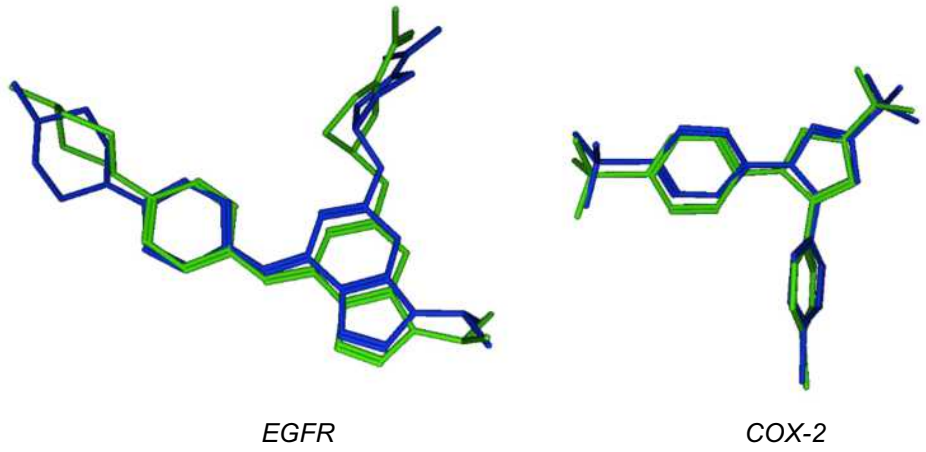

Figure 2 3D representation of the superimposed co-crystallized conformers (Blue sticks) and docked conformers (green sticks).

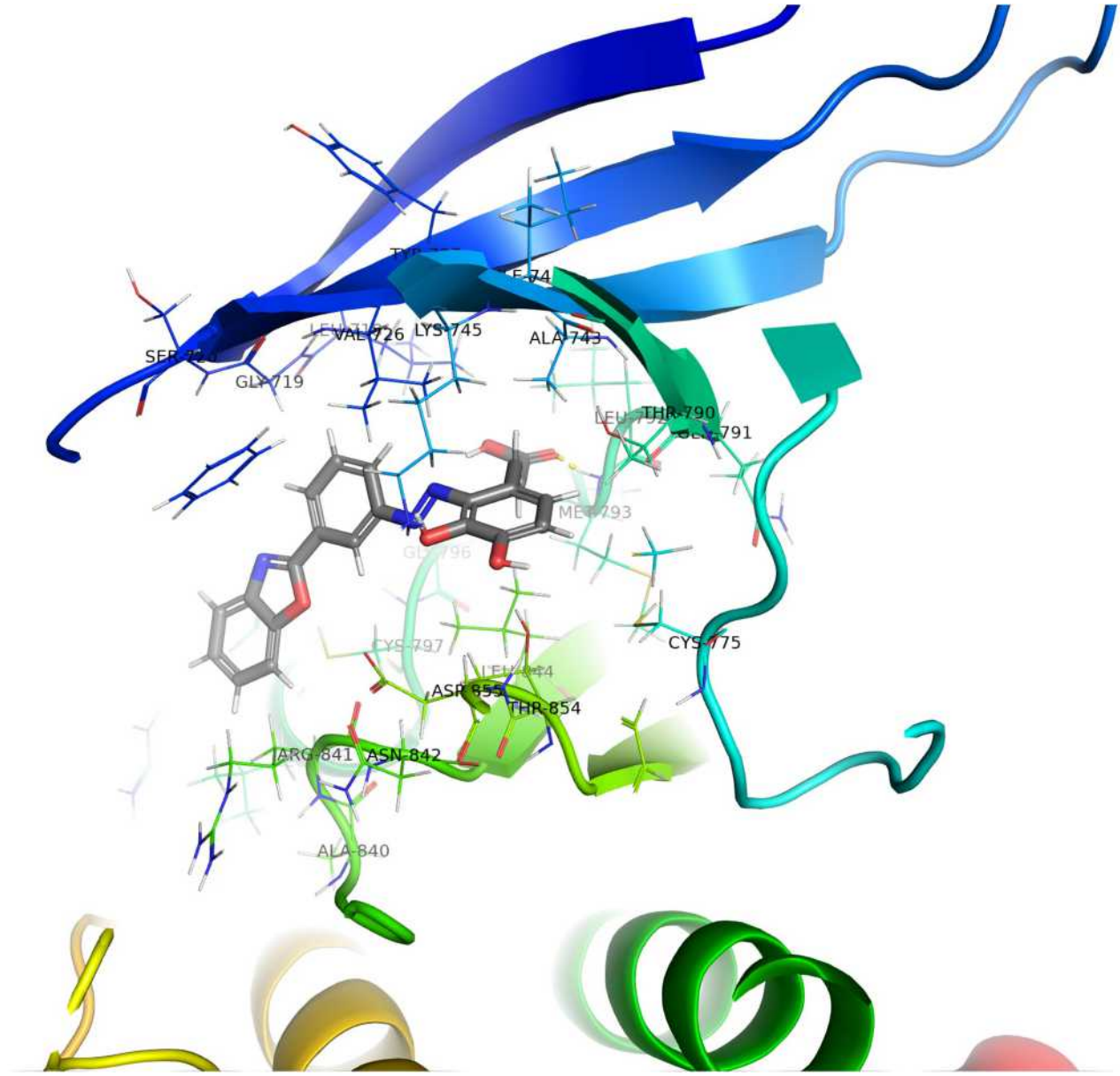

Figure 3 Predicted 3D demonstration of binding modes of C4 inside the active site of EGFR (PDB ID: 5UGB).

compounds **G1–G4** were shown effective as sPLA2-V inhibitors, with IC_{50} values ranging from 5.68 to 8.47μM. Among all semi-synthesized derivatives, **G4** was the most effective sPLA2-V inhibitor with IC_{50}: 5.68±0.54 μM. The scaffold containing gallic acid showed the strongest activity, especially when combined with benzoxazole moiety (**G4**, IC_{50}; 5.68uM). While the in vitro COX inhibitory activity of semi-synthetic derivatives was estimated by using a commercially available kit.[40] In this assay, the concentration of tested derivatives was 40 μg/mL. The IC_{50} values are displayed in Table 2. Research implicates, some derivatives have a selective affinity towards COX-1 while others have COX-2 affinity. **G1** and **G2** demonstrated potent COX-1 inhibition with IC_{50} in the range of 3.13 and 2.19 μM, respectively. Nevertheless, derivatives **C3, C4**, and **G3** showed moderate inhibitory activity against COX-1. In contrast, the other derivatives showed weak or without inhibitory action towards COX-1. The inhibitory action of azo- derivatives against COX-2 demonstrated that **G4** is a potent COX-2 inhibitor (IC_{50}, 2.47 μM, with SI 3.99), compared to standard indomethacin (IC_{50}: 3.25

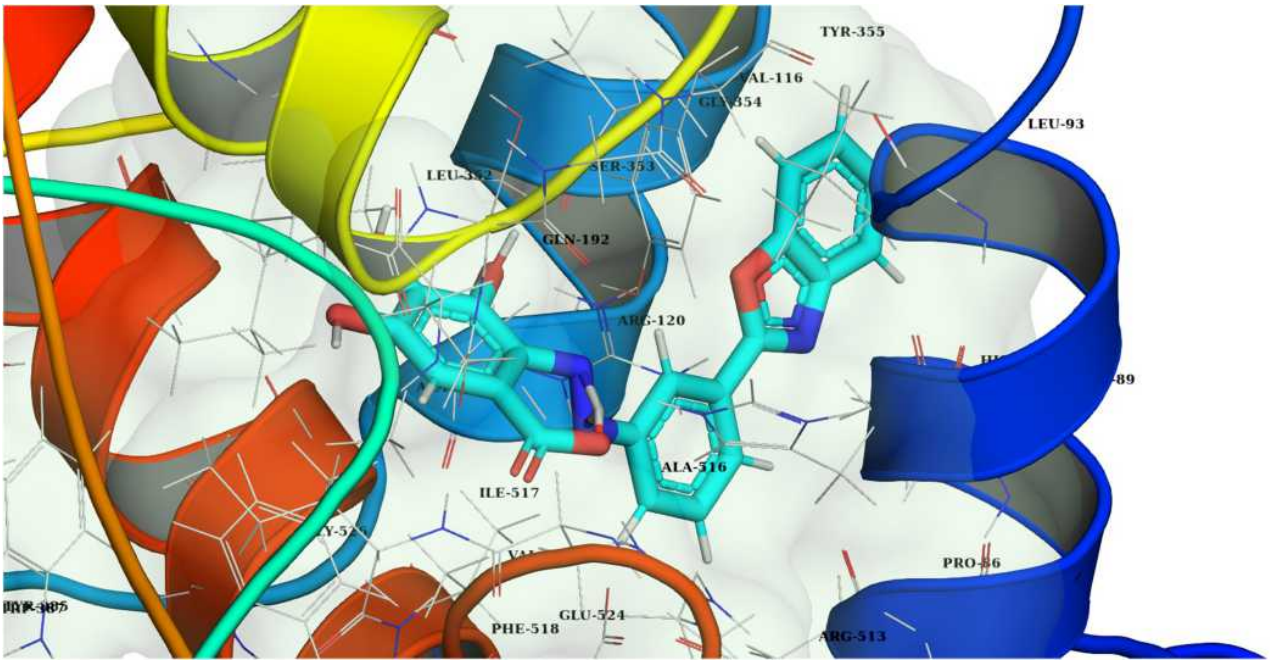

Figure 4 The Predicted 3D demonstration of binding modes of G4 inside the active site of COX-2 (PDB ID: 1CX2).

μM with SI of 0.084). The other compounds showed moderate to weak activity against COX-2 despite the SI of the compounds is being high.[17,44]

Inhibition of Interleukin 6 (IL-6) and Tumor Necrosis Factor- Alpha (TNF-α) Release in Lipopolysaccharide (LPS)-Stimulated Macrophages

In the current study, the inhibitory activity of **G2–G4** against LPS-triggered TNF-α and IL-6 release was evaluated in mouse macrophages (RAW264.7). To 10 μM of compounds **G2** to **G4**, the macrophages were added and subjected to incubation for 2h. To each well, LPS (0.5 μg/mL) was added and followed by 22h incubation. The amount of TNF-α and IL-6 was estimated by applying an enzyme-linked immunosorbent assay (ELISA). Table 2 shows the results of the anti-inflammatory test and all tested compounds were able to inhibit LPS-triggered IL-6 and TNF-α expression to various levels, exhibiting the maximum inhibition (32–61%) and (29–56) against LPS-triggered expression of TNF-α and IL-6, respectively. **G4** displayed the highest inhibition percentage of LPS-stimulated IL-6 and TNF-α (56 and 61%), respectively, as compared to LPS control.

Virtual C4 and G4 Docking

Molecular modelling studies were applied to check the plausible-binding interactions between the newly synthesized compounds and their potential targets. At first, the docking protocols were validated to get more reliable data. The validation based on re-docking the co-crystallized ligands imitated the same binding modes of the co-crystallized ligands with root-mean-square deviation (RMSD) values of 1.2 and 0.58 for EGFR and COX-2 receptors, respectively. Figure 2 depicts that much similarity exists between the co-crystallized and docked conformer of co-crystallized ligand.

The docking results showed that **C4** has an energy score of −13.8376 Kcal/mol (less than ligand 8BM energy score of −11.250 Kcal/mol) and binds with EGFR (5UGB) through HB with Met793 amino acid, which is the same amino acid binder of the ligand 8BM.[45,46] However, the docking of **G4** with COX-2 protein (1CX2) demonstrated five interactions; four of them are HBs and one arene-cation interaction. The HBs of **G4** with 1CX2 formed between amino acid residue His90, Tyr355, Ser530, Ser530 and Arg513 with N-imidazole, C=O, 3-OH, and 4-OH, respectively (Figures 3 and 4).[12,19] Compared to the ligand bromocelecoxib, **G4** formed five interactions; one H bond with His90 amino acid (a main amino acid in the

pocket) with an energy score of −24.1500 Kcal/mol, however, the ligand displays only one HB with an energy score of −13.8924 Kcal/mol. The highest COX-2 inhibitory activity of the benzoxazole-gallic acid scaffold is attributed to the benzoxazole moiety's large hydrophobic volume (Table 4).

Conclusions

Most of the target semi-synthetic products showed moderate to potent dual inhibitory activity against EGFR and COX-2 inhibitory activities. The coupling between benzoxazole moiety with caffeic acid in one scaffold displayed potent cytotoxic and kinase inhibitory activity for both EGFR and BRAF, while the scaffold of benzoxazole with gallic acid demonstrated COXs inhibitory actions and showed anti-inflammatory activity. Docking studies, which aligned with the biological evaluations, displayed that the energy scores are lower than for both EGFR and COX-2 enzymes also, the G4 demonstrated more interactions than the bromocelecoxib. The Nitrogen of benzoxazole and benzimidazole moieties has important role in binding with both COX 2 and EGFR enzymes through HB.

Acknowledgments

The authors extend their appreciation to the Deanship of Scientific Research at Jouf University for funding this work through research grant No (DSR-2021-01-0103). The authors would like to extend their sincere appreciation to Taif University for funding this project through the Researchers Supporting program, (Project number TURSP-2020/208), Taif University, Taif, Saudi Arabia. Also, the authors thank AlMarrefa, University, Ad Diriyah, 13713, Saudi Arabia for support and Dr Ahmed Khames for his evert in reviewing and editing manuscript.

Disclosure

The authors reported no conflicts of interest for this work.

References

1. Lee KW, Kim YJ, Lee HJ, Lee CY. Cocoa has more phenolic phytochemicals and a higher antioxidant capacity than teas and red wine. *J Agric Food Chem*. 2003;51:7292–7295. doi:10.1021/jf0344385
2. Habauzit V, Horcajada M-N. Phenolic phytochemicals and bone. *Phytochem Rev*. 2008;7(2):313–344. doi:10.1007/s11101-007-9078-9
3. Al-Saikhan M, Howard L, Miller JJ. Antioxidant activity and total phenolics in different genotypes of potato (Solanum tuberosum, l.). *J Food Sci*. 1995;60:341–343. doi:10.1111/j.1365-2621.1995.tb05668.x
4. Izli G. Total phenolics, antioxidant capacity, colour and drying characteristics of date fruit dried with different methods. *Food Sci Technol*. 2017;37:139–147. doi:10.1590/1678-457x.14516
5. Jiang F, Dusting GJ. Natural phenolic compounds as cardiovascular therapeutics: potential role of their antiinflammatory effects. *Curr Vasc Pharmacol*. 2003;1:135–156. doi:10.2174/1570161033476736
6. Abdallah HM, Esmat A. Antioxidant and anti-inflammatory activities of the major phenolics from zygophyllum simplex l. *J Ethnopharmacol*. 2017;205:51–56. doi:10.1016/j.jep.2017.04.022
7. Nohynek LJ, Alakomi H-L, Kähkönen MP, et al. Berry phenolics: antimicrobial properties and mechanisms of action against severe human pathogens. *Nutr Cancer*. 2006;54:18–32. doi:10.1207/s15327914nc5401_4
8. Zacchino SA, Butassi E, Di Liberto M, Raimondi M, Postigo A, Sortino M. Plant phenolics and terpenoids as adjuvants of antibacterial and antifungal drugs. *Phytomedicine*. 2017;37:27–48.
9. Vinayagam R, Jayachandran M, Xu B. Antidiabetic effects of simple phenolic acids: a comprehensive review. *Phytother Res*. 2016;30:184–199. doi:10.1002/ptr.5528
10. Gomes CA, Girão da Cruz T, Andrade JL, Milhazes N, Borges F, Marques MPM. Anticancer activity of phenolic acids of natural or synthetic origin: a Structure−Activity Study. *J Med Chem*. 2003;46(25):5395–5401. doi:10.1021/jm030956v
11. Xu M, Rao J, Chen B. Phenolic compounds in germinated cereal and pulse seeds: classification, transformation, and metabolic process. *Crit Rev Food Sci Nutr*. 2020;60(5):740–759. doi:10.1080/10408398.2018.1550051
12. Ghoneim MM, Musa A, El-Hela AA, Elokely KM. Evaluation and understanding the molecular basis of the antimethicillin-resistant staphylococcus aureus activity of secondary metabolites isolated from lamium amplexicaule. *Pharmacogn Mag*. 2018;14(55):3. doi:10.4103/pm.pm_541_17
13. Mahmoud BK, Hamed AN, Samy MN, et al. Phytochemical composition and antimicrobial properties of markhamia platycalyx (baker) sprague leaf. *Trop J Pharm Res*. 2019;18:2623–2631.
14. Zhang J, Yang PL, Gray NS. Targeting cancer with small molecule kinase inhibitors. *Nat Rev Cancer*. 2009;9(1):28–39. doi:10.1038/nrc2559
15. Kannaiyan R, Mahadevan D. A comprehensive review of protein kinase inhibitors for cancer therapy. *Expert Rev Anticancer Ther*. 2018;18(12):1249–1270. doi:10.1080/14737140.2018.1527688
16. Shen F-Q, Wang Z-C, Wu S-Y, et al. Synthesis of novel hybrids of pyrazole and coumarin as dual inhibitors of cox-2 and 5-lox. *Bioorg Med Chem Lett*. 2017;27(16):3653–3660. doi:10.1016/j.bmcl.2017.07.020
17. Abdelgawad MA, Bakr RB, Ahmad W, Al-Sanea MM, Elshemy HAH. New pyrimidine-benzoxazole/benzimidazole hybrids: synthesis, antioxidant, cytotoxic activity, in vitro cyclooxygenase and phospholipase a2-v inhibition. *Bioorg Chem*. 2019;92:103218. doi:10.1016/j.bioorg.2019.103218
18. Alkahtani HM, Abdalla AN, Obaidullah AJ, et al. Synthesis, cytotoxic evaluation, and molecular docking studies of novel quinazoline derivatives with benzenesulfonamide and anilide tails: dual inhibitors of egfr/her2. *Bioorg Chem*. 2020;95:103461. doi:10.1016/j.bioorg.2019.103461
19. Musa A, Al-muaikel NS, Abdel-Bakky MS. Phytochemical and pharmacological evaluations of ethanolic extract of bassia eriophora. *Der Pharma Chem*. 2016;8:169–178.
20. Musa A. Chemical constituents, antimicrobial and antiinflammatory evaluations of various extracts ofsuaeda vera forssk. Growing in Saudi Arabia. *Int J Pharm Res*. 2019;11:962–967.
21. Saldaña-Rivera L, Bello M, Méndez-Luna D. Structural insight into the binding mechanism of ATP to EGFR and L858R, and T790M and L858R/T790 mutants. *J Biomol Struct Dyn*. 2019;37(17):4671–4684. doi:10.1080/07391102.2018.1558112

22. Bello M, Saldaña-Rivero L, Correa-Basurto J, García B, Sánchez-Espinosa VA. Structural and energetic basis for the molecular recognition of dual synthetic vs. Natural inhibitors of egfr/her2. *Int J Biol Macromol*. 2018;111:569–586. doi:10.1016/j.ijbiomac.2017.12.162
23. El-Sayed NA, Nour MS, Salem MA, Arafa RK. New oxadiazoles with selective-cox-2 and egfr dual inhibitory activity: design, synthesis, cytotoxicity evaluation and in silico studies. *Eur J Med Chem*. 2019;183:111693. doi:10.1016/j.ejmech.2019.111693
24. Abdelgawad MA, Bakr RB, Alkhoja OA, Mohamed WR. Design, synthesis and antitumor activity of novel pyrazolo [3, 4-d] pyrimidine derivatives as egfr-tk inhibitors. *Bioorg Chem*. 2016;66:88–96. doi:10.1016/j.bioorg.2016.03.011
25. Araki K, Hashimoto K, Ardyanto TD, et al. Co-expression of cox-2 and egfr in stage i human bronchial adenocarcinomas. *Lung Cancer*. 2004;45(2):161–169. doi:10.1016/j.lungcan.2004.01.013
26. Youssif BG, Abdelrahman MH, Abdelazeem AH, et al. Design, synthesis, mechanistic and histopathological studies of small-molecules of novel indole-2-carboxamides and pyrazino [1, 2-a] indol-1 (2h)-ones as potential anticancer agents effecting the reactive oxygen species production. *Eur J Med Chem*. 2018;146:260–273. doi:10.1016/j.ejmech.2018.01.042
27. Shawky AM, Abourehab MA, Abdalla AN, Gouda AM. Optimization of pyrrolizine-based schiff bases with 4-thiazolidinone motif: design, synthesis and investigation of cytotoxicity and anti-inflammatory potency. *Eur J Med Chem*. 2020;185:111780. doi:10.1016/j.ejmech.2019.111780
28. Benelli R, Venè R, Minghelli S, Carlone S, Gatteschi B, Ferrari N. Celecoxib induces proliferation and amphiregulin production in colon subepithelial myofibroblasts, activating erk1–2 signaling in synergy with egfr. *Cancer Lett*. 2013;328:73–82. doi:10.1016/j.canlet.2012.09.008
29. Abdelgawad MA, Abdellatif KR, Ahmed OM. Design, synthesis and anticancer screening of novel pyrazole derivatives linking to benzimidazole, benzoxazole and benzothiazole. *Med Chem S*. 2014;1:2161–2444.
30. Abdelgawad MA, Bakr RB, El-Gendy AO, Kamel GM, Azouz AA, Bukhari SNA. Discovery of a cox-2 selective inhibitor hit with anti-inflammatory activity and gastric ulcer protective effect. *Future Med Chem*. 2017;9:1899–1912. doi:10.4155/fmc-2017-0115
31. Abdelgawad MA, Belal A, Ahmed OM. Synthesis, molecular docking studies and cytotoxic screening of certain novel thiazolidinone derivatives substituted with benzothiazole or benzoxazole. *J Chem Pharm Res*. 2013;5:318–327.
32. Abdelgawad MA, Mohamed AM, Musa A, Mostafa EM, Awad HM. Synthesis, chromatographic separation and antimicrobial evolution of new azoquinoline-8-ol. *J Pharm Sci Res*. 2018;10:1314–1318.
33. Gao X, Kuo J, Jiang H, et al. Immunomodulatory activity of curcumin: suppression of lymphocyte proliferation, development of cell-mediated cytotoxicity, and cytokine production in vitro. *Biochem Pharmacol*. 2004;68:51–61. doi:10.1016/j.bcp.2004.03.015
34. Gao X, Xu YX, Janakiraman N, Chapman RA, Gautam SC. Immunomodulatory activity of resveratrol: suppression of lymphocyte proliferation, development of cell-mediated cytotoxicity, and cytokine production. *Biochem Pharmacol*. 2001;62:1299–1308. doi:10.1016/S0006-2952(01)00775-4
35. Al-Sanea MM. Synthesis and biological evaluation of small molecule modulators of cdk8/cyclin c complex with phenylaminoquinoline scaffold. *PeerJ*. 2020;8:e8649. doi:10.7717/peerj.8649
36. Al-Sanea M, Abdelazem A, Park B, et al. Ros1 kinase inhibitors for molecular-targeted therapies. *Curr Med Chem*. 2016;23:142–160. doi:10.2174/0929867322666151006093623
37. Pohanka M, Hrabinova M, Kuca K. Diagnosis of intoxication by the organophosphate vx: comparison between an electrochemical sensor and ellman´ s photometric method. *Sensors*. 2008;8:5229–5237. doi:10.3390/s8095229
38. Ahmad W, Kumolosasi E, Jantan I, Bukhari SN, Jasamai M. Effects of novel diarylpentanoid analogues of curcumin on secretory phospholipase a2, cyclooxygenases, lipo-oxygenase, and microsomal prostaglandin e synthase-1. *Chem Biol Drug Des*. 2014;83:670–681. doi:10.1111/cbdd.12280
39. Bukhari SNA, Lauro G, Jantan I, Bifulco G, Amjad MW. Pharmacological evaluation and docking studies of α, β-unsaturated carbonyl based synthetic compounds as inhibitors of secretory phospholipase a2, cyclooxygenases, lipoxygenase and proinflammatory cytokines. *Bioorg Med Chem*. 2014;22:4151–4161. doi:10.1016/j.bmc.2014.05.052
40. Jantan I, Bukhari SNA, Adekoya OA, Sylte I. Studies of synthetic chalcone derivatives as potential inhibitors of secretory phospholipase a2, cyclooxygenases, lipoxygenase and pro-inflammatory cytokines. *Drug Des Devel Ther*. 2014;8:1405. doi:10.2147/DDDT.S67370
41. Gogos CA, Drosou E, Bassaris HP, Skoutelis A. Pro-versus anti-inflammatory cytokine profile in patients with severe sepsis: a marker for prognosis and future therapeutic options. *J Infect Dis*. 2000;181:176–180. doi:10.1086/315214
42. Al-Sanea MM, Elkamhawy A, Paik S, et al. Sulfonamide-based 4-anilinoquinoline derivatives as novel dual aurora kinase (aurka/b) inhibitors: synthesis, biological evaluation and in silico insights. *Bioorg Med Chem*. 2020;28:115525. doi:10.1016/j.bmc.2020.115525
43. Al-Sanea MM, Park BS, Abdelazem AZ, et al. Optimization of bipyridinyl pyrazole scaffolds via design, synthesis and screening of a new series of ros1 kinase-modulating compounds. *Bull Korean Chem Soc*. 2015;36:305–311. doi:10.1002/bkcs.10077
44. Kaur A, Pathak DP, Sharma V, Wakode S. Synthesis, biological evaluation and docking study of a new series of di-substituted benzoxazole derivatives as selective cox-2 inhibitors and anti-inflammatory agents. *Bioorg Med Chem*. 2018;26:891–902. doi:10.1016/j.bmc.2018.01.007
45. Mostafa EM, Gamal M, Ghoneim MM, et al. Repurposing of FDA approved alkaloids as covid 19 inhibitors; in silico studies. *Pharmacogn J*. 2021;13.
46. Alkhaldi AA, Musa A, Mostafa EM, Amin E, De Koning HP. Docking studies and antiprotozoal activity of secondary metabolites isolated from scrophularia syriaca benth. Growing in Saudi Arabia. *Rec Nat Prod*. 2020;14:30.